



Swansea University
Prifysgol Abertawe



Cronfa - Swansea University Open Access Repository

This is an author produced version of a paper published in :
Carbohydrate Polymers

Cronfa URL for this paper:

<http://cronfa.swan.ac.uk/Record/cronfa26367>

Paper:

Powell, L., Khan, S., Chinga-Carrasco, G., Wright, C., Hill, K. & Thomas, D. (2016). An investigation of *Pseudomonas aeruginosa* biofilm growth on novel nanocellulose fibre dressings. *Carbohydrate Polymers*, 137, 191-197.

<http://dx.doi.org/10.1016/j.carbpol.2015.10.024>

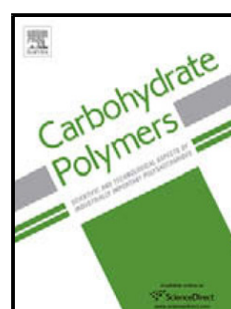
This article is brought to you by Swansea University. Any person downloading material is agreeing to abide by the terms of the repository licence. Authors are personally responsible for adhering to publisher restrictions or conditions. When uploading content they are required to comply with their publisher agreement and the SHERPA RoMEO database to judge whether or not it is copyright safe to add this version of the paper to this repository.

<http://www.swansea.ac.uk/iss/researchsupport/cronfa-support/>

Accepted Manuscript

Title: An investigation of *Pseudomonas aeruginosa* biofilm growth on novel nanocellulose fiber dressings

Author: Lydia C. Powell Saira Khan Gary Chinga-Carrasco
Chris J. Wright Katja E. Hill David W. Thomas



PII: S0144-8617(15)01004-8
DOI: <http://dx.doi.org/doi:10.1016/j.carbpol.2015.10.024>
Reference: CARP 10441

To appear in:

Received date: 15-6-2015
Revised date: 18-9-2015
Accepted date: 9-10-2015

Please cite this article as: Powell, L. C., Khan, S., Chinga-Carrasco, G., Wright, C. J., Hill, K. E., and Thomas, D. W., An investigation of *Pseudomonas aeruginosa* biofilm growth on novel nanocellulose fiber dressings, *Carbohydrate Polymers* (2015), <http://dx.doi.org/10.1016/j.carbpol.2015.10.024>

This is a PDF file of an unedited manuscript that has been accepted for publication. As a service to our customers we are providing this early version of the manuscript. The manuscript will undergo copyediting, typesetting, and review of the resulting proof before it is published in its final form. Please note that during the production process errors may be discovered which could affect the content, and all legal disclaimers that apply to the journal pertain.

Intended for submission to *Carbohydrate polymers*. Last update 150918. GCH.

1 **Highlights**

2 Nanocellulose has shown potential usefulness in advanced wound dressing applications.

3 Nanocellulose had the ability to form smooth, translucent films.

4 The ability of nanocellulose to impair bacterial growth was assessed.

5 Nanocellulose demonstrated impaired biofilm growth compared to the Aquacel[®] control.

6 Cells exhibited altered morphology when grown on nanocellulose compared to Aquacel[®].

7

8

9

10

11 **An investigation of *Pseudomonas aeruginosa* biofilm growth on novel nanocellulose**
12 **fiber dressings.**

13 Lydia C. Powell^{a,b}, Saira Khan^a, Gary Chinga-Carrasco^{c,*}, Chris J. Wright^b, Katja E. Hill^a,
14 David W. Thomas^a.

15 ^aAdvanced Therapies Group, College of Biomedical and Life Sciences, Cardiff University
16 School of Dentistry, Cardiff, CF14 4XY, UK;

17 ^bCentre for NanoHealth, Systems and Process Engineering Centre, College of Engineering,
18 Swansea University, Swansea, SA2 8PP, UK;

19 ^cPaper and Fibre Research Institute (PFI), NO-7491 Trondheim, Norway.

20 ***Corresponding author.** Tel: +47 45412304

21 E-mail address: gary.chinga.carrasco@pfi.no

22 **ABSTRACT**

23 Nanocellulose from wood is a novel biomaterial, which is highly fibrillated at the nanoscale.

24 This affords the material a number of advantages, including self-assembly, biodegradability

Intended for submission to *Carbohydrate polymers*. Last update 150918. GCH.

25 and the ability to absorb and retain moisture, which highlights its potential usefulness in
26 clinical wound-dressing applications. In these *in vitro* studies, the wound pathogen
27 *Pseudomonas aeruginosa* PAO1 was used to assess the ability of two nanocellulose materials
28 to impair bacterial growth (<48 h). The two nanocelluloses had a relatively small fraction of
29 residual fibres (<4%) and thus a large fraction of nanofibrils (widths<20 nm). Scanning
30 electron microscopy and confocal laser scanning microscopy imaging demonstrated impaired
31 biofilm growth on the nanocellulose films and increased cell death when compared to a
32 commercial control wound dressing, Aquacel[®]. Nanocellulose suspensions inhibited
33 bacterial growth, whilst UV-vis spectrophotometry and laser profilometry also revealed the
34 ability of nanocellulose to form smooth, translucent films. Atomic force microscopy studies
35 of the surface properties of nanocellulose demonstrated that PAO1 exhibited markedly
36 contrasting morphology when grown on the nanocellulose film surfaces compared to an
37 Aquacel[®] control dressing ($p<0.05$). This study highlights the potential utility of these
38 biodegradable materials, from a renewable source, for wound dressing applications in the
39 prevention and treatment of biofilm development.

40 **Keywords: Nanocellulose, Biofilm, *Pseudomonas aeruginosa*, Atomic Force Microscopy,**
41 **Characterisation**

42

43 **1. Introduction**

44 Human wound healing represents a complex sequence of inter-related and overlapping
45 biological events. When the skin is disrupted, a series of processes are triggered to restore
46 barrier function, prevent water loss and reduce the risk of bacterial invasion of the deeper
47 tissues. Disruption of these processes and failure to heal is unfortunately frequent, and is
48 estimated to occur in >60% of the population. These “chronic wounds” represent an
49 important and unrecognised cause of morbidity and mortality and are estimated in the US
50 alone to cost \$25 billion annually (Gottrup, 2004; Gjødsbøl et al., 2006; Sen et al., 2009). In
51 an attempt to reduce water-loss from the wound surface, decrease bacterial contamination and
52 promote healing, specialist dressings have been employed as standard care for these wounds
53 (Boateng et al., 2008); this market was estimated in 2011 to be, worth \$12.8 billion
54 (Transparency Market Research, 2013). Increasingly, rather than being solely “simple” inert
55 barriers, these dressings possess impregnated biological functions, which have ranged from
56 antimicrobials (e.g. silver/iodine) to anti-inflammatory components (e.g. oxidised cellulose).
57 Dressings have also been used to deliver cell-based therapies (e.g. fibroblasts) with varying
58 degrees of success (Veves, Sheehan, & Pham, 2002; Atiyeh et al., 2007; Boateng et al.,
59 2008). The ideal dressing material would have the following properties: water loss control
60 (to maintain a moist environment); high mechanical strength, elasticity and conformability;
61 ability to inhibit bacterial growth and biodegradability (Sai & Babu, 2000; Kokabi,
62 Sirousazar & Hassan, 2007). Possession of innate antibacterial properties is particularly
63 useful for dressing materials as all wounds harbour bacteria which may directly, or indirectly
64 inhibit wound healing and stimulate chronic inflammation within the wound bed (Gjødsbøl et
65 al., 2006; Bjarnsholt et al., 2008; James et al., 2008).

66 Cellulose is the most abundant organic polymer on Earth. In attempting to deliver novel
67 materials, researchers have developed nanocellulose structures derived from a variety of
68 sources including, wood, annual crops and agricultural residues (Wågberg et al., 2008; Saito
69 et al., 2009; Syverud et al., 2010; Klemm et al., 2011; Jonoobi et al., 2012; Alila et al., 2013).
70 Nanocellulose is therefore, renewable, biodegradable and obtained from sustainable non-oil
71 based resources (Dufresne, 2013).

72 In the production process, the resultant nanofibrillar structures can be produced using a
73 variety of pre-treatments, including applying 2,2,6,6-tetramethylpiperidine-1-oxyl (TEMPO)-
74 mediated oxidation, carboxymethylation, periodate oxidation; generating nanofibrillar

Intended for submission to *Carbohydrate polymers*. Last update 150918. GCH.

75 structures with distinct structural and chemical properties (Saito et al., 2006; Wågberg et al.,
76 2008; Liimatainen et al., 2012). The nanocellulose structures produced with chemical pre-
77 treatments are usually composed of nanofibrils with a narrow diameter distribution, generally
78 less than 20 nm (Saito et al., 2006, Saito et al., 2009; Chinga-Carrasco et al., 2011) in contrast
79 to those produced without chemical pre-treatment. Cellulose nanofibrils possess a high
80 aspect-ratio and surface area, with resultant high tensile strength and modulus (Saito et al.,
81 2013; Josselson et al., 2015).

82 In recent years, there has been a growing interest in harnessing the potential of this
83 abundant renewable resource as a valuable nanomaterial for biomedical applications (Lin &
84 Dufresne, 2014; Jorfi & Foster, 2015). The use of oxidized nanofibrils for cross-linking to
85 generate elastic cryo-gels with a desired pore size, demonstrated the potential of these
86 materials for use in dressing materials, potentially facilitating wound fluid absorption and
87 controlled drug release (Syverud et al., 2011b; Chinga-Carrasco & Syverud, 2014; Rees et al.,
88 2015). Importantly, nanocellulose materials have been demonstrated to be non-cytotoxic
89 against a series of cell-lines (Vartianen et al., 2011; Dong et al., 2012; Alexandresku et al.,
90 2013).

91 These studies characterized the interaction of the known wound pathogen *Pseudomonas*
92 *aeruginosa* with nanocellulose materials derived from *Pinus radiata* pulp fibres.
93 *Pseudomonas* spp. are one of the most common colonisers of non-healing wounds, being
94 found in up to 80% of chronic venous leg ulcers (Davies et al., 2004). The ability of the
95 materials to support *P. aeruginosa* growth in suspension and on nanocellulose films was
96 screened to determine whether these nanoscale materials possessed any distinct, size-
97 dependent antimicrobial properties when compared to the commercial wound dressing,
98 Aquacel[®]. The surface and optical properties of nanocellulose films were also assessed to
99 determine its suitability in wound dressing applications.

100

101 **2. Materials and methods**

102 **2.1. Nanocellulose materials**

103 Bleached *P. radiata* pulp fibers that were elemental chlorine -free (ECF) kraft market
104 pulp were selected for use in this study. Bleached pulp fibres were pre-treated with TEMPO-
105 mediated oxidation according to Syverud et al. (2011a). The pulp fibres were homogenized
106 with a Rannie 15 type 12.56 X homogenizer, operated at 1000 bar pressure, where the pulp

Intended for submission to Carbohydrate polymers. Last update 150918. GCH.

107 consistency during homogenizing was 0.5%. The oxidized fibrillated materials were
108 collected after 1 and 2 passes through the homogenizer and labelled T01 and T02
109 respectively. The nanocellulose materials were then diluted in deionised water to 0.4% w/v
110 before subsequent use. The fraction of residual fibres in the T01 and T02 nanocelluloses was
111 quantified with a FiberMaster device, as described by Chinga-Carrasco et al. (2014). The
112 typical diameter of similar cellulose nanofibrils from the same pulp-fibre raw material has
113 been reported to be less than 20 nm (Chinga-Carrasco et al., 2011), with the ability to form
114 low-porosity films with density higher than 1300 kg/m³ (Chinga-Carrasco & Syverud, 2012).
115 The carboxyl and aldehyde content have been quantified to be 855 and 71 µmol/g cellulose,
116 respectively (Rees et al., 2015).

117 **2.2. Screening for the ability to impair PAO1 growth**

118 To screen for bacterial contamination, autoclaved nanocellulose suspensions were
119 supplemented with Mueller Hinton broth (MHB) (50%, v/v), with phosphate buffered saline
120 (PBS; 50%, v/v) being used as the control. The suspensions were incubated at 37°C and the
121 growth (optical density) monitored over 24 hours at 600 nm (OD₆₀₀) in a FLUOstar Optima
122 plate reader (BMG LABTECH). The ability of nanocellulose to impair bacterial growth was
123 also examined by inoculating identical suspensions with an overnight culture of *P.*
124 *aeruginosa* PAO1 and again monitoring growth (optical density) over 24 hours as described
125 above.

126 **2.3. Surface characterization of nanocellulose films**

127 Air-dried nanocellulose films (20 g/m²) were produced from T01 and T02 autoclaved
128 nanocellulose suspensions (0.4% w/v). The microstructural surface of the films was
129 characterized by laser profilometry (LP). Ten LP topography images (1 mm × 1 mm) were
130 acquired from the top and underside surfaces of each film sample, using a lateral and z-
131 resolution of 1 µm and 10 nm, respectively. The surface images were bandpass-filtered to
132 enable quantification of the surface topography. ImageJ software (National Institutes of
133 Health) and the SurfCharJ plugin were used for image processing and analysis to achieve
134 roughness values described by the root-mean square (RMS), as previously described (Chinga-
135 Carrasco et al., 2014). Additionally, the optical properties of the films were assessed with a
136 UV-vis spectrophotometer (Cary 300 Conc, Varian). The wavelengths between 200 and 800
137 nm were included for analysis. Three replicates were measured for each series. The
138 nanostructure of the films was characterized using atomic force microscopy (AFM). AFM

Intended for submission to *Carbohydrate polymers*. Last update 150918. GCH.

139 imaging was performed using a Dimension 3100 AFM (Bruker) in tapping-mode operation in
140 air to achieve image sizes of $50 \mu\text{m}^2$ and image resolution of 1024×1024 pixels.

141 Solubility and sorption tests of the nanocellulose films were adapted from Parr &
142 Rueggeberg (2002). Briefly, T01 and T02 nanocellulose films (2 cm^2) were first desiccated
143 for 24 hours and weighed, before being placed into 5 ml of de-ionised water at 37°C for 24 h.
144 Excess water from the sample surface was then removed with absorbent paper and the
145 nanocellulose samples re-weighed. Samples were placed into a desiccator again for 24 hours
146 and before being weighed again. Water sorption and solubility were then calculated as
147 previously described Parr & Rueggeberg (2002).

148 **2.4. Characterization of bacterial growth on air-dried nanocellulose films**

149 The ability of T01 and T02 air-dried nanocellulose films to impair biofilm growth was
150 compared to growth on a commercial wound dressing, Aquacel[®] (ConvaTec, USA).
151 Aquacel[®] is a clinical hydrofiber wound dressing made from sodium carboxymethylcellulose.
152 T01 and T02 films (2 cm^2) and Aquacel[®] (2 cm^2) were placed individually within a six-well
153 plate with MHB and inoculated with an overnight culture of *P. aeruginosa* PAO1 and
154 incubated at 37°C for 24 h. For AFM imaging, the biofilms were gently rinsed twice to
155 remove planktonic bacteria and allowed to air dry before imaging. A Dimension 3100 AFM
156 (Bruker) was used to achieve AFM images, using tapping-mode operation in air and a scan
157 speed of approximately 1 Hz. For confocal laser scanning microscopy (CLSM) imaging, the
158 films were gently rinsed once after 24 or 48 hours growth, stained with LIVE/DEAD[®]
159 BacLight[™] Bacterial Viability Kit (Invitrogen, Paisley, UK) containing SYTO 9 dye and
160 propidium iodide and set in Vectashield (Vector Laboratories, UK), prior to being imaged
161 under an Olympus Fluoview FV1000 CLSM. For SEM imaging, the supernatant was
162 removed at 24 and 48 hours and each well immersed in 2.5% glutaraldehyde and then washed
163 thoroughly with distilled water. One ml of distilled water was added to each well and
164 biofilms frozen (at -20°C). Once frozen, the well plates were then freeze-dried for 24 hours.
165 The films were imaged at 1 kV using an Hitachi S4800 SEM.

166 **2.5. Cell Viability from Nanocellulose surfaces**

167 T01 and T02 nanocellulose films, a glass slide and Aquacel[®], each 2 cm^2 in size, were
168 incubated at 37°C in MHB after inoculation with an overnight culture of *P. aeruginosa*
169 PAO1. After 24 hours growth, films were placed into 5 ml PBS to remove loosely adherent
170 bacteria. This wash step was then repeated. Films were then vortexed in fresh PBS for 5

Intended for submission to *Carbohydrate polymers*. Last update 150918. GCH.

171 mins to remove attached bacteria and the suspension used to prepare triplicate serial dilutions
172 and drop counts (3 x 20 μ l per dilution) on dried blood agar plates and incubated overnight at
173 37°C, before counting colonies forming units (cfu).

174 2.6 Statistics

175 The level of significant differences in this study were determined using the Mann-
176 Whitney U test, where a p value of <0.05 was considered significant.

177

178 3. Results and discussion

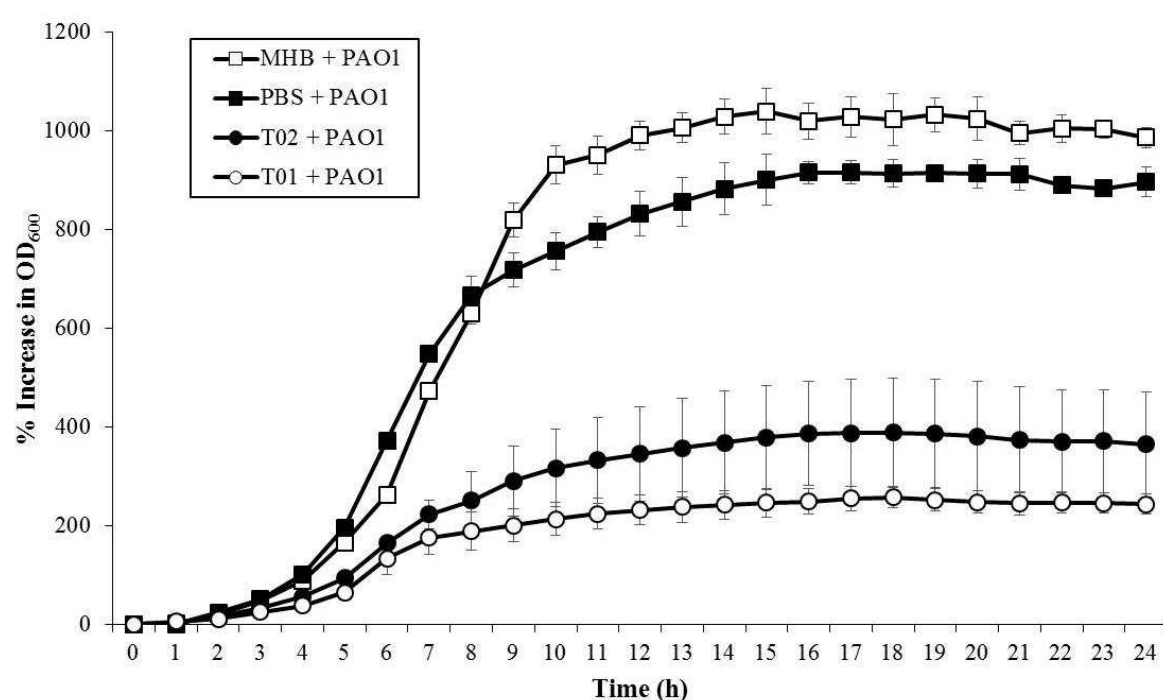
179 These studies utilized growth curve assays, cell viability assays, CLSM, SEM and AFM
180 techniques to determine whether these nanocellulose materials possessed antimicrobial
181 properties for wound dressing applications. The nanocellulose suspensions used were first
182 pre-treated with TEMPO-mediated oxidation, which led to region-specific oxidation of the
183 C6-position, introducing carboxyl groups and small numbers of aldehyde groups (Saito et al.,
184 2006). The oxidation of the pulp facilitates the fibrillation of the cellulose fibers in the
185 homogenization process, leading to a high yield of cellulose nanofibrils (Chinga-Carrasco et
186 al., 2011; Fukuzumi, Saito & Isogai, 2013). The effect of these highly-fibrillated
187 nanocellulose materials on the growth of *P. aeruginosa* will be assessed in the following
188 sections.

189 3.1. Growth of *Pseudomonas aeruginosa* PAO1 in nanocellulose suspensions

190 Optical density measurements of autoclaved T01 and T02 nanocellulose suspension
191 supplemented with MHB revealed no bacterial growth (data not shown) and hence that no
192 inherent bacterial contamination was present in these samples. In contrast, growth curves of
193 nanocellulose suspensions inoculated with PAO1 showed that they appeared to support the
194 growth of this strain over 24 hours (Fig. 1), with the greatest bacterial biomass observed in
195 the T02 nanocellulose suspension material (366 ± 107 OD₆₀₀ at 24h) and slightly less seen in
196 the T01 suspension (244 ± 20 OD₆₀₀ at 24h). However, compared to the inoculated PBS and
197 MHB controls, growth of *P. aeruginosa* PAO1 in the presence of the nanocellulose
198 suspensions was greatly reduced. In addition, the un-inoculated PBS- and MHB-only
199 controls showed no change in optical density over 24 h, remaining at 0 for each time point
200 (data not shown). Therefore, the initial growth curve assays demonstrated that the

Intended for submission to *Carbohydrate polymers*. Last update 150918. GCH.

201 nanocellulose materials did not appear to promote bacterial growth, (compared to both
 202 inoculated controls where growth was strong due to the added MHB); reassuringly
 203 confirming that *P. aeruginosa* PAO1 does not use the nanocellulose as a carbon source. In
 204 fact, it was apparent that the nanocellulose materials actually inhibited growth as similar
 205 growth curves to that of the inoculated PBS control would otherwise have been expected.
 206 The extent of this inhibition varied with the extent of fibrillation of the material being tested.
 207 The less fibrillated material T01 contained a larger fraction of residual fibres ($3.5 \pm 0.2\%$)
 208 due to only one homogenization pass (see also Fig. 2), imposing a slightly greater inhibitory
 209 effect on planktonic PAO1 growth than the more fibrillated material T02 which contained
 210 less residual fibres ($1.3 \pm 0.1\%$) and thus a larger fraction of nanofibrils due to two
 211 homogenization passes (see also Chinga-Carrasco et al., 2014). As the number of
 212 homogenization cycles appears to have a direct effect on planktonic bacterial growth, this
 213 may have possible implications for the future development of these materials in medical
 214 applications.



215
 216 **Fig. 1.** Optical density (OD₆₀₀) of 24 hour *Pseudomonas aeruginosa* PAO1 growth in
 217 nanocellulose suspensions (T01 and T02). MHB, Mueller-Hinton Broth; PBS, phosphate
 218 buffered saline.

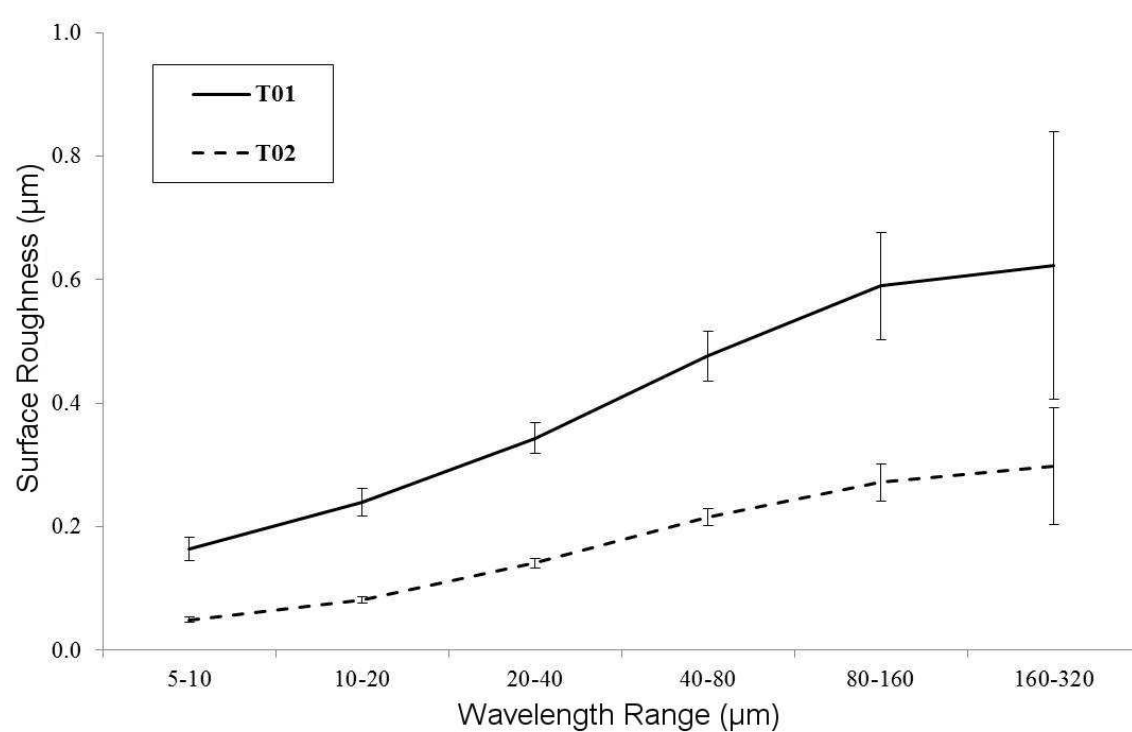
219

Intended for submission to Carbohydrate polymers. Last update 150918. GCH.

220 3.2. Characterization of the structural properties of nanocellulose films

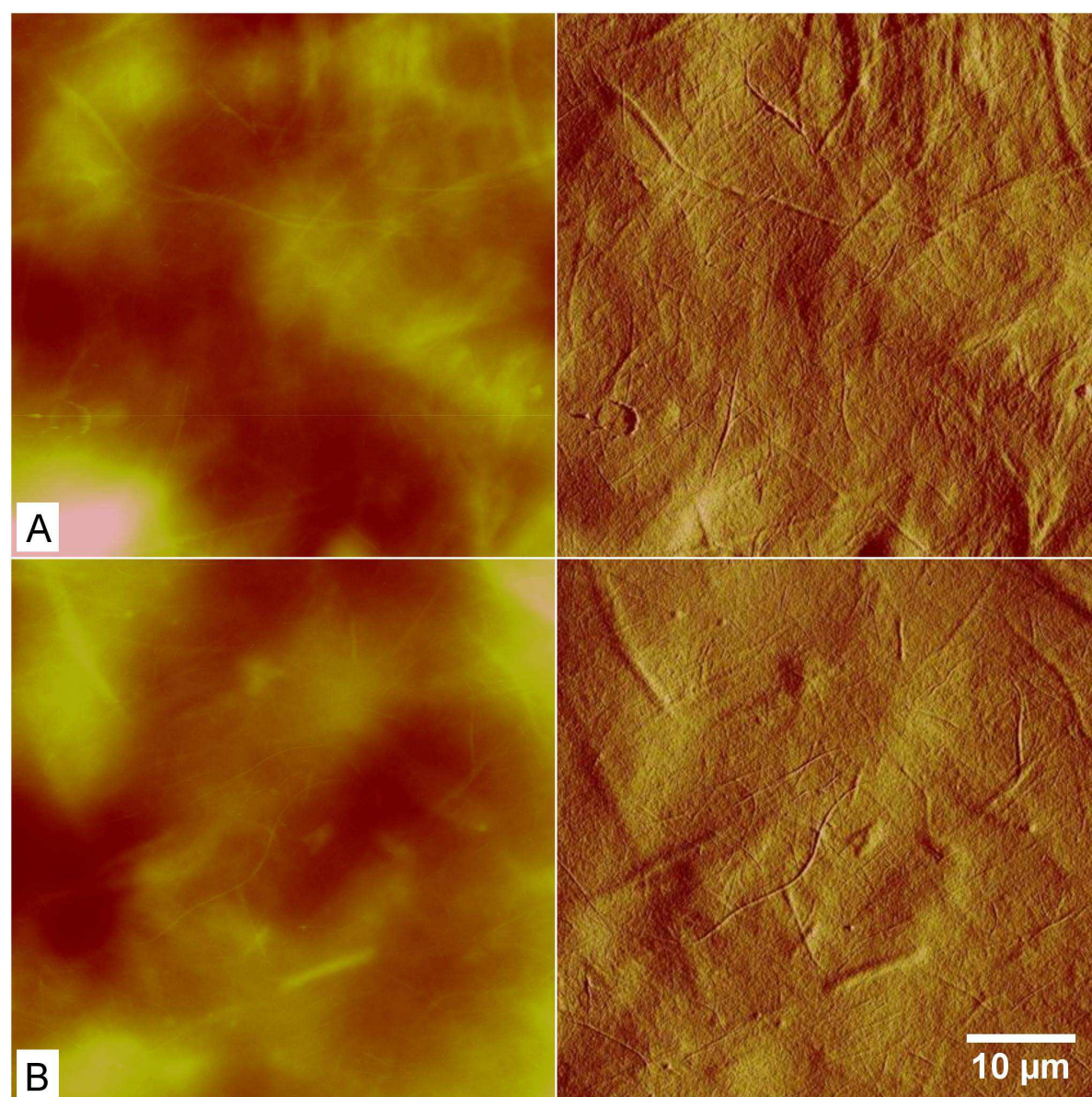
221 To assess nanocellulose as a potential wound dressing material, films were prepared by
222 air-drying and these rudimentary films were tested for relevant physical properties. The
223 surface roughness of the films, assessed at the micrometre scale with LP (Fig. 2), revealed
224 that the T02 film was significantly smoother than the T01 ($0.53 \pm 0.04 \mu\text{m}$ vs, $1.25 \pm 0.1 \mu\text{m}$
225 respectively; $p < 0.05$). This result was confirmed (but not significantly so) by the difference
226 also observed in the surface roughness measurements obtained from the AFM images ($273 \pm$
227 128 nm vs. $392 \pm 146 \text{ nm}$, respectively; $p = 0.069$) (Fig. 3). Hence, the surface roughness
228 quantification revealed the relatively smooth surfaces for both materials, with the roughness
229 assessed at several wavelengths indicative of a high degree of fibrillation of the material
230 (Chinga-Carrasco & Syverud, 2014).

231



232 **Fig. 2.** Laser profilometry (LP) analysis of nanocellulose films (T01 and T02). Mean values
233 of $n=10$ determinations \pm standard deviations.
234

Intended for submission to Carbohydrate polymers. Last update 150918. GCH.

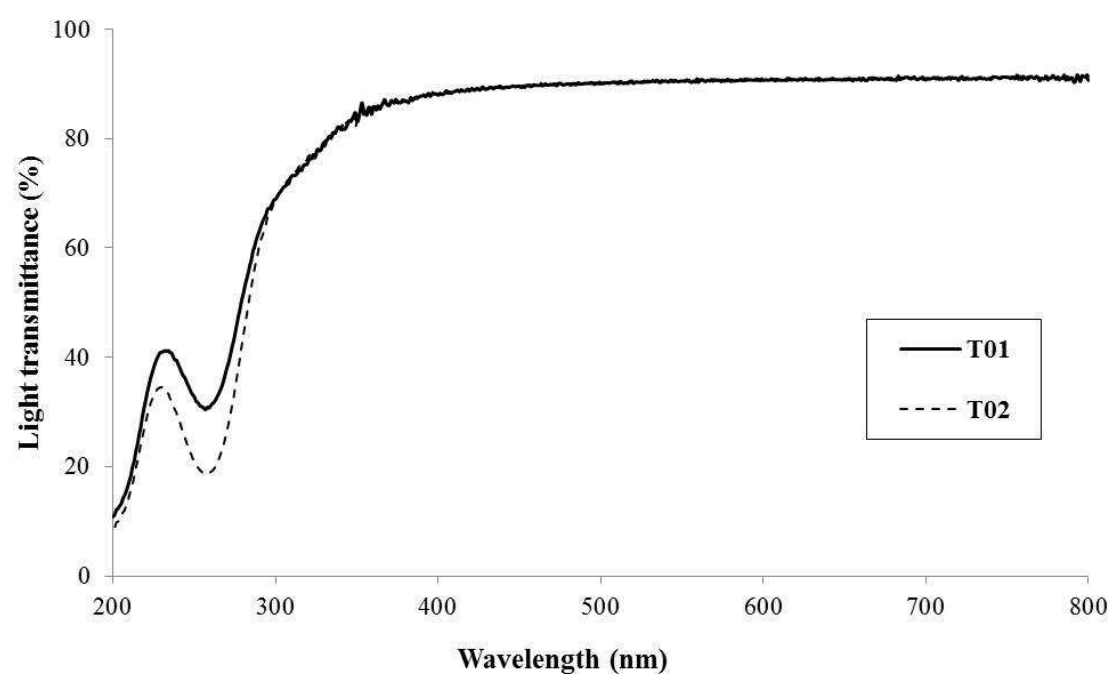


235
236 **Fig. 3.** Atomic force microscopy (AFM) imaging of nanocellulose films. AFM
237 topographical (left) and amplitude (right) imaging of (A) T01 (Z-height = 2 μm) and (B) T02
238 (Z-height = 1.5 μm) respectively. (Scale bar is 10 μm).

239
240 Interestingly, both the T02 and T01 nanocellulose films revealed very high water
241 sorption values (2232 ± 113 % vs. 2153 ± 22 % respectively) most likely due to their high
242 surface area to volume ratio and highly absorbent nature. Solubility values of the T01 and
243 T02 nanocellulose films were low (15.1 ± 3.2 % vs. 15.6 ± 1.8 % respectively). No
244 significant differences were found between T01 and T02 films for either water sorption and
245 solubility ($p > 0.05$).

Intended for submission to *Carbohydrate polymers*. Last update 150918. GCH.

246 In addition, T01 and T02 nanocellulose films, characterized by UV vis
247 spectrophotometry, were found to possess a high degree of light transmittance (91% at a
248 wavelength of 650 nm; Fig. 4) confirming the high degree of fibrillation in the materials.
249 T01 and T02 nanocellulose materials thus formed films with a high degree of light
250 transmittance, due to the dense packing of the nanofibers, and fissures between the fibers
251 (Nogi et al., 2009). High translucency of the films can be a great advantage for wound
252 dressing applications, as the wound bed could potentially be monitored by visual inspection
253 without the need for the removal of the dressing from the wound.
254



255
256 **Fig. 4.** Light transmittance using UV Vis spectrophotometry of air-dried T01 and T02
257 nanocellulose films (n=3).

258
259 The TEMPO-mediated oxidation modified the surface of cellulose nanofibrils,
260 introducing both carboxyl (855 $\mu\text{mol/g}$) and aldehyde groups (71 $\mu\text{mol/g}$) (Rees et al., 2014).
261 The occurrence of aldehyde groups was confirmed by the “shoulders” at bands between 200
262 and 300 nm (Fukuzumi et al., 2009). The T02 sample had a more pronounced decrease of
263 light transmittance at the 200-300 nm band, probably indicative of a larger number of
264 exposed aldehyde groups due to the high nanofibrillation of this material (see also Chinga-
265 Carrasco, 2013).

Intended for submission to *Carbohydrate polymers*. Last update 150918. GCH.

266 These carboxyl and aldehyde groups could be used to add functionality to the material
267 (Chinga-Carrasco and Syverud, 2014). This ability to modify nanocellulose materials to
268 covalently bond biomodulatory agents (e.g. growth factors or quaternary ammonium
269 compounds), suggests that it may be possible to combine the physical properties of
270 nanocellulose films (i.e. high surface area to volume ratio and small pore size) with
271 antimicrobials (Andresen et al., 2007). Such modification of nanocellulose materials with
272 antimicrobials is however, not necessarily beneficial; surface-modified nanocellulose with
273 quaternary ammonium compounds having previously been shown to be cytotoxic
274 (Alexandresku et al., 2013).

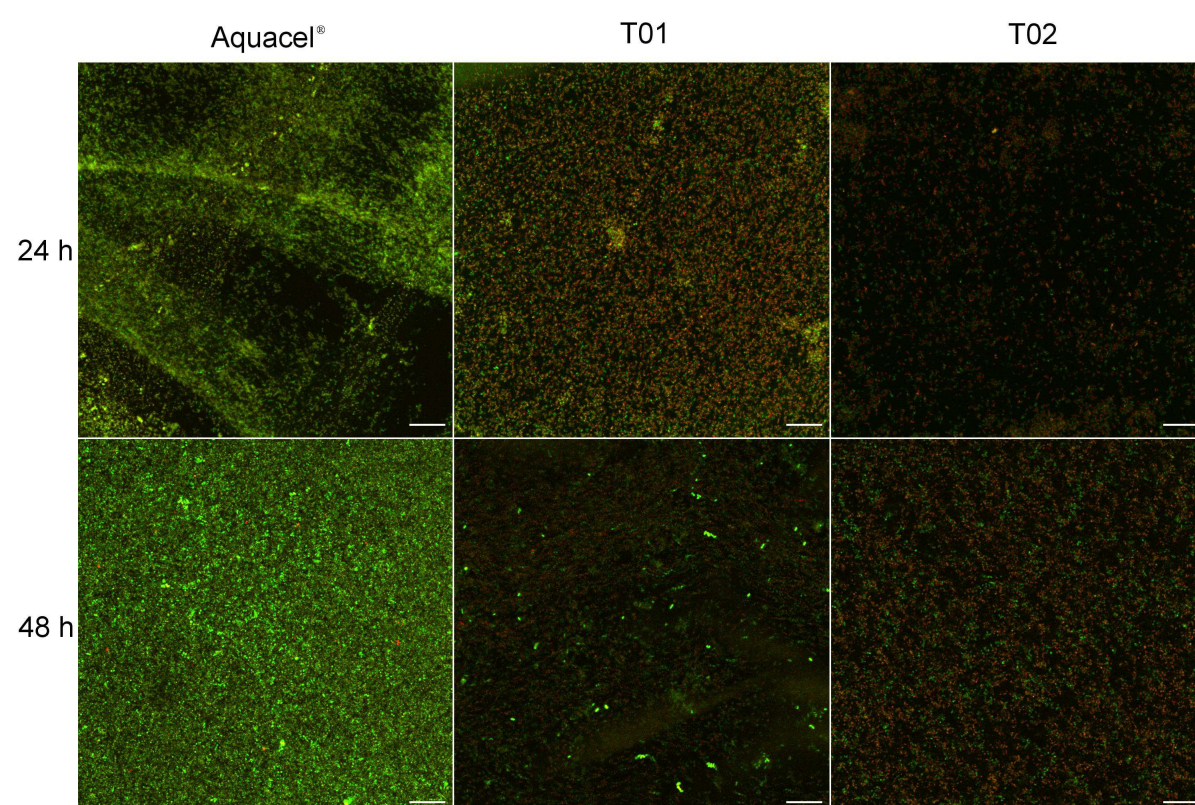
275

276 3.3. *Bacterial biofilm growth on dried nanocellulose films*

277 Within chronic wounds, bacteria exist as biofilms, tightly adhering to material and host-
278 tissue surfaces, rather than as “free-floating” (planktonic) bacteria (Bjarnsholt et al., 2008;
279 Hill et al., 2010). It was, therefore, important, to determine the ability of the nanocellulose
280 materials to support biofilm growth. In these experiments, we studied the physical
281 interaction of the bacteria and subsequent biofilm formation with the film surface using a
282 variety of imaging techniques and quantified biofilm cell viability on the film surfaces in
283 comparison to the commercially-available dressing Aquacel[®]. Whilst, CLSM and SEM have
284 been employed to examine bacterial and *Candida* growth on wound dressings (Newman et
285 al., 2006; Tran et al., 2009; Anghel et al., 2013), AFM has attracted relatively little attention
286 (Oh et al., 2009; Wright et al., 2010).

287 CLSM imaging with LIVE/DEAD[®] staining demonstrated less bacterial growth on the
288 T01 and T02 nanocellulose materials and more cell death when compared to Aquacel[®], for
289 both 24 and 48 hours growth (Fig. 5). Decreased PAO1 biofilm growth was thus evident on
290 the nanocellulose materials. The observed biofilm clusters corresponded with SEM imaging,
291 which revealed that PAO1 adherence and growth resulted in distinct clusters of bacterial cells
292 on the nanocellulose materials when compared to Aquacel[®]. In addition, the biofilm clusters
293 on both films appeared to be considerably more developed at 48 hours than 24 hours (Fig. 6).

Intended for submission to *Carbohydrate polymers*. Last update 150918. GCH.



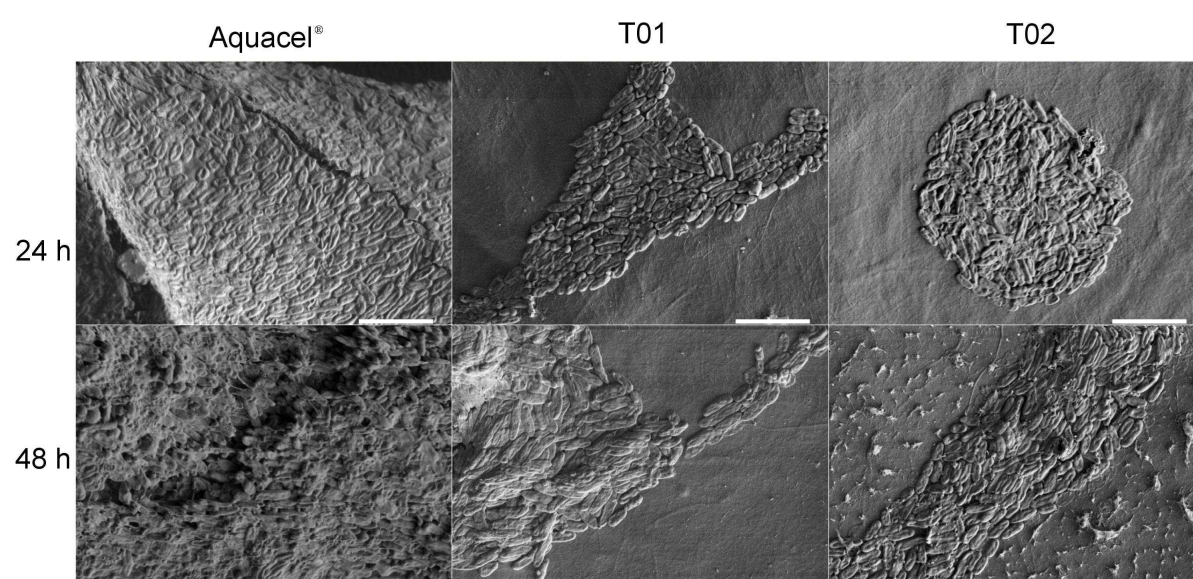
294

295 **Fig. 5.** Confocal laser scanning microscopy (CLSM) imaging of 24 and 48 hour
296 *Pseudomonas aeruginosa* PAO1 growth on T01 and T02 nanocellulose films and Aquacel®
297 using LIVE/DEAD® staining, showing live (green) and non-vital cells (red). (Scale bar = 20
298 μm).

299

300 Aquacel® itself demonstrated greater bacterial coverage seen throughout the material for
301 both 24 and 48 hours compared to either of the nanocellulose materials (Fig. 6). A previous
302 study revealed that the bacterial population in contact with a Hydrofiber® (Aquacel®)
303 dressing could maintain viability for at least 21 hours (Newman et al., 2006). Comparing the
304 nanocellulose materials to this non-antimicrobial, commercially used, wound dressing,
305 showed distinct differences, with the nanocellulose appearing to possess inherent anti-
306 microbial properties.

Intended for submission to *Carbohydrate polymers*. Last update 150918. GCH.



307

308 **Fig. 6.** Scanning electron microscopy imaging of 24 and 48 hour *Pseudomonas aeruginosa*
 309 PAO1 growth on T01 and T02 nanocellulose film surfaces and within the lower, more fibrous
 310 Aquacel® dressing layer. (Scale bar = 5 μm).

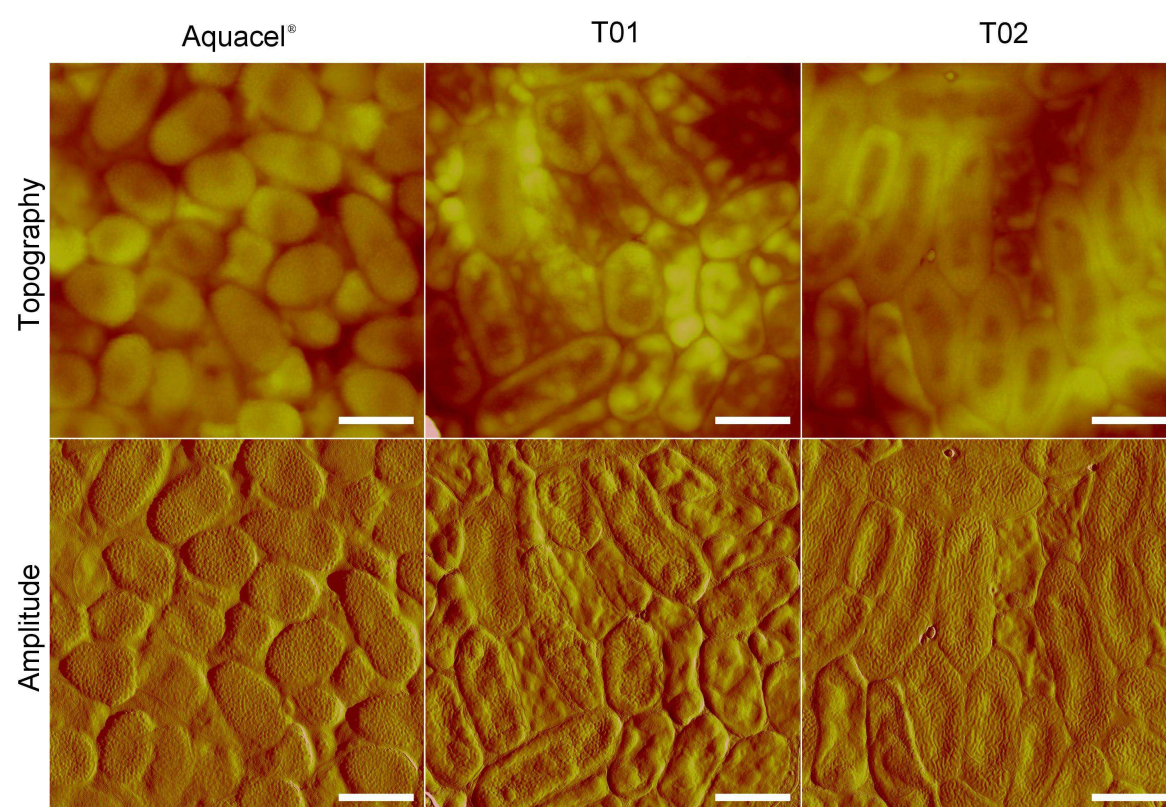
311

312 Under conditions of hydration, Aquacel® forms a cohesive gelled surface where the
 313 material under the surface remains more fibrous and less gel-like, giving two distinctly
 314 different environments for bacterial growth. This smooth amorphous gel surface can make it
 315 difficult to discern bacterial cells or fibres using SEM imaging (Walker et al., 2003). In
 316 contrast, bacterial cells growing under this gelled surface (in the more fibrous dressing
 317 material) can be more readily visualised with SEM imaging, but only through cracks in the
 318 Aquacel® surface, as also demonstrated in this study.

319 In contrast to SEM, AFM is able to more fully map the surface topography of a material,
 320 giving a 3-dimensional image of higher magnification. Therefore, AFM was employed to
 321 give an enhanced view of the surface structure of the smooth Aquacel® gel sample and the
 322 T01 and T02 materials (**Fig. 7**). Interestingly, the PAO1 cells exhibited a very different
 323 morphology in the biofilm on the Aquacel® surface, in that the cells were significantly
 324 smaller in length (1.02 ± 0.18 vs. 1.61 ± 0.37 μm ; $p < 0.05$) and had a less wrinkled
 325 appearance compared to those on the nanocellulose materials. The gelled surface of
 326 Aquacel® may offer an altered micro-environment for bacterial growth, not present in the
 327 novel nanocellulose materials, which could have resulted in these observed differences.
 328 Furthermore, the cells on the Aquacel® appeared less ‘stressed’ compared to those growing
 329 on the T01 and T02 materials, perhaps due to nutritional stress on the latter, which is known

Intended for submission to *Carbohydrate polymers*. Last update 150918. GCH.

330 to induce cell filamentation (elongation). In contrast, SEM imaging of the bacterial cells
 331 below the gelled surface (in the more fibrous Aquacel[®] dressing material) did not exhibit this
 332 altered morphology when compared to the nanocellulose films.
 333



334
 335 **Fig. 7.** Atomic force microscopy imaging of 24 hour *Pseudomonas aeruginosa* PAO1 growth
 336 on the T01 and T02 nanocellulose film surfaces and Aquacel[®] dressing surface. (Scale bar =
 337 1 μ m).

338

339 Cell viability studies showed no significant difference in cell numbers (CFU/mL)
 340 between either the T01 (1.7×10^8), T02 (1.2×10^8) or Aquacel[®] (2.5×10^8) surfaces, whilst
 341 the glass slide control showed significantly less bacterial attachment (2×10^6 ; $p < 0.05$). The
 342 similar cell viability between the materials was possibly due to the previously described
 343 gelling properties of Aquacel[®] (Walker et al., 2003). Even though CLSM confirmed
 344 increased and indeed confluent biofilm growth on the Aquacel[®], this was not reflected in the
 345 viability counts. Aquacel[®] has been shown to encapsulate populations of pathogenic bacteria
 346 under its gelled surface, providing an ideal environment to immobilise them (Walker et al.,

Intended for submission to *Carbohydrate polymers*. Last update 150918. GCH.

347 2003) and the vortexing used in this study was clearly insufficient to release all the bacterial
348 cells from the dressing material for the viability assay.

349 Although in suspension, T01 showed better bacterial growth impairment than T02,
350 interestingly, no difference in biofilm growth was evident between the films with CLSM,
351 AFM and SEM. The two experiments assessed different modes of bacterial growth;
352 planktonic versus biofilm, and on different media (liquid and solid) thereby accounting for
353 the differences seen. When the nanocellulose is in film form, other properties become
354 important for bacterial attachment and growth, such as surface roughness, which is irrelevant
355 in suspension.

356

357

358 **4. Conclusions**

359 The results of this study highlight the potential usefulness of nanocellulose, from a
360 renewable source. They demonstrate that whilst these bio-degradable materials were not
361 utilised as a carbon-source to support bacterial growth of *P. aeruginosa*, they instead are able
362 to effectively inhibit bacterial growth. The ability to control the physical material properties
363 e.g. tensile strength, surface roughness and translucency, as well as the ability to covalently
364 link therapeutic compounds to their surface, has many applications in wound healing and
365 surgery.

366

367 **Conflict of interest**

368 There are no conflicts of interest to report.

369

370 **Acknowledgements**

371 This work has been funded by the Research Council of Norway through the NANO2021
372 program, grant no. 219733 – NanoHeal: Bio-compatible cellulose nanostructures for
373 advanced wound healing applications.

374

375 **References**

376 Alexandresku, L., Syverud, K., Gatti, A. & Chinga-Carrasco, G. (2013). Cytotoxicity tests
377 of cellulose nanofibril-based structures. *Cellulose* 20, 1765-1775.

Intended for submission to *Carbohydrate polymers*. Last update 150918. GCH.

- 378 Alila, S., Besbes, I., Rei Vilar, M., Mutjé, P., Boufi, S. (2013). Non-woody plants as raw
379 materials for production of microfibrillated cellulose (MFC): A comparative study.
380 *Industrial Crops & Products* 41, 250– 259.
- 381 Andresen, M., Stenstad, P., Møretrø, T., Langsrud, S., Syverud, K., Johansson, L-S. &
382 Stenius, P. (2007). Nonleaching antimicrobial films prepared from surface-modified
383 microfibrillated cellulose. *Biomacromolecules* 8, 2149-2155.
- 384 Anghel, I., Holban, AM., Andronescu, E., Grumezescu, AM. & Chifiriuc, MC. (2013).
385 Efficient surface functionalization of wound dressings by a phytoactive nanocoating
386 refractory to *Candida albicans* biofilm development. *Biointerphases* 8, 12.
- 387 Atiyeh, BS., Costagliola, M., Hayek, SN. & Dibo, SA. (2007). Effect of silver on burn
388 wound infection control and healing: Review of the literature. *Burns* 33, 139-148.
- 389 Bjarnsholt, T., Kirketerp-Møller, K., Jensen, PØ., Madsen, KG., Phipps, R., Krogh, K.,
390 Høiby, N. & Givskov, M. (2008). Why chronic wounds will not heal: a novel hypothesis.
391 *Wound Repair & Regeneration* 16, 2-10.
- 392 Boateng, JS., Matthews, KH., Stevens, HNE., Eccleston, GM. (2008). Wound healing
393 dressings and drug delivery systems: a review. *Journal of Pharmaceutical Sciences* 97,
394 2892-2923.
- 395 Chinga-Carrasco, G., Yu, Y. & Diserud, O. (2011). Quantitative electron microscopy of
396 cellulose nanofibril structures from *Eucalyptus* and *Pinus radiata* kraft pulp fibres.
397 *Microscopy & Microanalysis* 17, 563-571.
- 398 Chinga-Carrasco, G. & Syverud, K. (2012). On the structure and oxygen transmission rate
399 of biodegradable cellulose nanobarriers. *Nanoscale Research Letters* 7, 192.
- 400 Chinga-Carrasco, G. (2013). Optical methods for the quantification of the fibrillation
401 degree of bleached MFC materials. *Micron*, 48: 42-48.
- 402 Chinga-Carrasco, G., Averianova, N., Kodalenko, O., Garaeva, M., Petrov, V., Leinsvang,
403 B. & Karlsen, T. (2014). The effect of residual fibres on the micro-topography of cellulose
404 nanopaper. *Micron* 56, 80-84.

Intended for submission to *Carbohydrate polymers*. Last update 150918. GCH.

- 405 Chinga-Carrasco, G. & Syverud, K. (2014). Pretreatment-dependent surface chemistry of
406 wood nanocellulose for pH-sensitive hydrogels. *Journal of Biomaterials Applications* 29,
407 423-432.
- 408 Davies, CE., Hill, KE., Wilson, MJ., Stephens, P., Hill, CM., Harding, KG. & Thomas,
409 DW. (2004). Use of 16S ribosomal DNA PCR and denaturing gradient gel electrophoresis
410 for analysis of the microfloras of healing and nonhealing chronic venous leg ulcers.
411 *Journal of Clinical Microbiology* 42, 3549-3557.
- 412 Dong, S., Hirani, AA., Colacino, KR., Lee, YW. & Roman, M. (2012). Cytotoxicity and
413 cellular uptake of cellulose nanocrystals. *Nano LIFE* 3, 1241006.
- 414 Dufresne, A. (2013). Nanocellulose: a new ageless bionanomaterial. *Materials Today* 16,
415 220-227.
- 416
- 417 Fukuzumi, H., Saito, T., Iwata, T., Kumamoto, Y. & Isogai, A. (2009). Transparent and
418 high gas barrier films of cellulose nanofibers prepared by TEMPO-mediated oxidation.
419 *Biomacromolecules* 10, 162-165
- 420
- 421 Fukuzumi, H., Saito, T. & Isogai, A. (2013). Influence of TEMPO-oxidized cellulose
422 nanofibril length on film properties. *Carbohydrate Polymers* 93, 172-177.
- 423 Gjødsbøl, K., Christensen, JJ., Karlsmark, T., Jørgensen, B., Klein, BM. & Kroghfelt, KA.
424 (2006). Multiple bacterial species reside in chronic wounds: a longitudinal study.
425 *International Wound Journal* 3, 225-231.
- 426 Gottrup, F. (2004). A specialized wound-healing centre concept: importance of a
427 multidisciplinary department structure and surgical treatment facilities in the treatment of
428 chronic wounds. *American Journal of Surgery* 187, 38S-43S.
- 429 Hill, KE., Malic, S., McKee, R., Rennison, T., Harding, KG., Williams, DW. & Thomas,
430 DW. (2010). An *in vitro* model of chronic wound biofilms to test wound dressings and
431 assess antimicrobial susceptibilities. *Journal of Antimicrobial Chemotherapy* 65, 1195-
432 1206.

Intended for submission to *Carbohydrate polymers*. Last update 150918. GCH.

- 433 James, GA., Swogger, E., Wolcott, R., Pulcini, Ed., Secor, P., Sestrich, J., Costerton, JW.
434 & Stewart, PS. (2008). Biofilms in chronic wounds. *Wound Repair & Regeneration* 16,
435 37-44.
- 436 Jonoobi, M., Mathew, A.P., & Oksman, K. (2012). Producing low-cost cellulose nanofiber
437 from sludge as new source of raw materials. *Industrial Crops & Products* 40, 232-238.
- 438 Jorfi, M. & Foster, E.J. (2015). Recent advances in nanocellulose for biomedical
439 applications. *Journal of Applied Polymer Science* 132, 41719.
- 440 Jossefson, G., Chinga-Carrasco, G. & Gamstedt, K. (2015). Elastic models coupling the
441 cellulose nanofibril to the macroscopic film level. *RSC Advances* 5, 58091-58099.
- 442 Klemm, D., Kramer, F., Moritz, S., Lindström, T., Ankerfors, M., Gray, D. & Dorris, A.
443 (2011). Nanocelluloses: A new family of nature-based materials. *Angewandte Chemie*
444 *International Edition* 50, 5438–5466.
- 445
- 446 Kokabi, M., Sirousazar, M. & Hassan, ZM. (2007). PVA-clay nanocomposite hydrogels
447 for wound dressing. *European Polymer Journal* 43, 773-781.
- 448 Liimatainen, H., Visanko, M., Sirviö, J., Hormi, OEO. & Niinimäki, J. (2012).
449 Enhancement of the nanofibrillation of wood cellulose strength through sequential
450 periodate-chlorite oxidation. *Biomacromolecules* 13, 1592–1597.
- 451 Lin, N. & Dufresne, A. (2014). Nanocellulose in biomedicine: Current status and future
452 prospect. *European Polymer Journal* 59, 302–325.
- 453 Newman, GR., Walker, M., Hobot, JA. & Bowler, PG. (2006). Visualisation of bacterial
454 sequestration and bactericidal activity within hydrating Hydrofiber wound dressings.
455 *Biomaterials* 27, 1129-1139.
- 456 Nogi, M., Iwamoto, S., Nakagaito, AN. & Yano, H. (2009). Optically transparent
457 nanofiber paper. *Advanced Materials* 21, 1595–1598.
- 458 Oh, YJ., Lee, NR., Jo, W., Jung, WK. & Lim, JS. (2009). Effects of substrates on biofilm
459 formation observed by atomic force microscopy. *Ultramicroscopy* 109, 874-880.

Intended for submission to *Carbohydrate polymers*. Last update 150918. GCH.

- 460 Parr, GR. & Rueggeberg, FA. (2002). *In vitro* hardness, water sorption and resin solubility
461 of laboratory-processed and autopolymerized long-term resilient denture liners over one
462 year of water storage. *Journal of Prosthetic Dentistry* 88, 139-144.
- 463 Rees, A., Powell, LC., Chinga-Carrasco, G., Gethin, DT., Syverud, K., Hill, KE. &
464 Thomas, DW. (2015). 3D Bioprinting of carboxymethylated-periodate oxidized
465 nanocellulose constructs for wound dressing applications. *BioMed Research International*
466 925757.
- 467 Sai, KP. & Babu, M. (2000). Collagen based dressings- a review. *Burns* 26, 54-62.
- 468 Saito, T., Nishiyama, Y., Putaux, JL., Vignon, M. & Isogai, A. (2006). Homogeneous
469 suspensions of individualized microfibrils from TEMPO-catalyzed oxidation of native
470 cellulose. *Biomacromolecules* 7, 1687-1691.
- 471 Saito, T., Hirota, M., Tamura, N., Kimura, S., Fukuzumi, H., Heux, L. & Isogai, A.
472 (2009). Individualization of nano-sized plant cellulose fibrils by direct surface
473 carboxylation using TEMPO catalyst under neutral conditions. *Biomacromolecules* 10,
474 1992-1996.
- 475 Saito, T., Kuramae, R., Wohler J., Berglund, L.A., & Isogai, A. (2013). An ultrastrong
476 nanofibrillar biomaterial: the strength of single cellulose nanofibrils revealed via
477 Sonication-Induced Fragmentation. *Biomacromolecules* 14, 248-253.
- 478 Sen, CK., Gordillo, GM., Roy, S., Kirsner, R., Lambert, L., Hunt, TK., Gottrup, F.,
479 Gurtner, GC. & Longaker, MT. (2009). Human skin wounds: A major and snowballing
480 threat to public health and the economy. *Wound Repair & Regeneration* 17, 763-771.
- 481 Syverud, K., Chinga-Carrasco, G., Toledo, J. & Toledo, P. (2011a). A comparative study
482 of Eucalyptus and *Pinus radiata* pulp fibres as raw materials for production of cellulose
483 nanofibrils. *Carbohydrate Polymers* 84, 1033-1038.
- 484 Syverud, K., Kirsebom, H., Hajizadeh, S. & Chinga-Carrasco, G. (2011b). Cross-linking
485 cellulose nanofibrils for potential elastic cryo-structured gels. *Nanoscale Research Letters*
486 6, 626.
- 487 Tran, PL., Hammond, AA., Mosley, T., Cortez, J., Gray, T., Colmer-Hamood, JA.,
488 Shashtri, M., Spallholz, JE., Havood, AN. & Reid, TW. (2009). Organoselenium coating

Intended for submission to *Carbohydrate polymers*. Last update 150918. GCH.

- 489 on cellulose inhibits the formation of biofilms by *Pseudomonas aeruginosa* and
490 *Staphylococcus aureus*. *Applied & Environmental Microbiology* 75, 3586-3592.
- 491 Transparency Market Research. (2013). Wound dressings market – global industry
492 analysis, size, share, trends, and forecast, 2012-2018.
- 493 Vartiainen, J., Pöhler, T., Sirola, K., Pylkkänen, L., Alenius, H., Hokkinen, J., Tapper, U.,
494 Lahtinen, P., Kapanen, A., Putkisto, K., Hiekkataipale, P., Eronen, P., Ruokolainen, J. &
495 Laukkanen, A. (2011). Health and environmental safety aspects of friction grinding and
496 spray drying of microfibrillated cellulose. *Cellulose* 18, 775–786.
- 497 Veves, A., Sheehan, P. & Pham, HT. (2002). A randomized, controlled trial of Promogran
498 (a collagen/oxidized regenerated cellulose dressing) vs standard treatment in the
499 management of diabetic foot ulcers. *Archives of Surgery* 137, 822-827.
- 500 Walker, M., Hobot, JA., Newman, GR. & Bowler, PG. (2003). Scanning electron
501 microscopic examination of bacterial immobilisation in a carboxymethyl cellulose
502 (AQUACEL) and alginate dressings. *Biomaterials* 24, 883-890.
- 503 Wright, CJ., Shah, MK., Powell, LC. & Armstrong, I. (2010). Application of AFM from
504 microbial cell to biofilm. *Scanning* 32, 134-149.
- 505 Wågberg, L., Decher, G., Norgren, M., Lindström, T., Ankerfors, M. & Axnäs, K. (2008).
506 The build-up of polyelectrolyte multilayers of microfibrillated cellulose and cationic
507 polyelectrolytes. *Langmuir* 24, 784–795.